A SIMPLE DESIGN APPROACH FOR UHPFRC IN BENDING

Torsten Leutbecher and Ekkehard Fehling

Institute of Structural Engineering, University of Kassel, Germany

Abstract

For economic design and construction of long-span structures made of UHPFRC as well as for the exploitation of the ultra high compressive strength in bending members in general, traditional reinforcement (rebar, prestressing) is needed in addition to the fibres. For the design of UHPFRC cross-sections with combined reinforcement subject to bending with/without axial force, the well-known assumptions and equilibrium conditions for designing reinforced and prestressed concrete have to be extended in order to consider the contribution of fibres.

For this purpose, a simplified design approach is discussed in this paper. After presenting material models suitable for cross-sectional design of UHPFRC, a well-founded engineering model is derived that is, in addition, easy to handle. For validation, the predictions of the model are compared with results from 4-point bending tests on UHPFRC beams with passive reinforcement.

Résumé

Pour la conception et la construction économique de structures de longue portée en BFUP, ainsi que pour l'exploitation de la ultra haute résistance à la compression dans des éléments de flexion, des armatures traditionnelles (ferraillage passif, emploi de précontrainte) sont en général nécessaire en plus des fibres. Pour la conception des sections en BFUP renforcées avec des armatures soumises à la flexion avec/sans force axiale, les hypothèses connues et les conditions d'équilibre pour la conception du béton armé et précontraint doivent être étendus afin d'examiner la contribution des fibres.

A cet effet, une approche de conception simplifiée est présentée dans cet article. Après d'avoir décrit les modèles de matériaux nécessaire pour le calcul de la section, un modèle d'ingénierie bien-fondé est dérivé qui est, en outre, facile à manipuler. Pour la validation, les prédictions du modèle sont comparées avec les résultats d'essais de flexion 4 point sur des poutres en BFUP avec un ferraillage passif.

1.   INTRODUCTION

The assumptions for the design of reinforced concrete and prestressed concrete subject to bending with/without axial force traditionally are as follows [1].

- plane sections remain plane.
- the strain in bonded reinforcement or bonded prestressing tendons, whether in tension or in compression, is the same as that in the surrounding concrete.
- the tensile strength of the concrete is ignored.
- the stresses in the concrete in compression as well as the stresses in the reinforcing or prestressing steel are derived from the relevant design stress-strain relationships.

These basic assumptions can be applied in principle also to the design of ultra high-strength concrete structures that are reinforced exclusively with conventional reinforcing steel using a representative stress-strain relation in compression.

However, when combining fibres and conventional reinforcement, the tensile forces in the cracked tensile zone are carried by both types of reinforcement mutually. Thus, enhancement of the above-mentioned design principles is necessary that will be discussed in detail in the following. Furthermore, a well-founded but simple engineering model is presented that can be used in cross-sectional design of UHPFRC subject to bending with/without axial force and that provides good agreement with test results of UHPFRC beams with passive reinforcement.

2.   MATERIAL MODELS FOR DESIGN OF UHPC CROSS-SECTIONS

2.1   Compression loading

UHPFRC behaves nearly linear elastic in uniaxial compression tests up to a stress level of approx. 85 to 90 % of the compressive strength. Regardless of the maximum particle size, the increase of deformations due to micro-cracking immediately before failure is only slightly pronounced. For cross-sectional design, this small nonlinearity can be neglected. Simplifying, linear elastic behaviour can be assumed until reaching the design value of the concrete compressive strength f_{cd} (see Fig. 1).
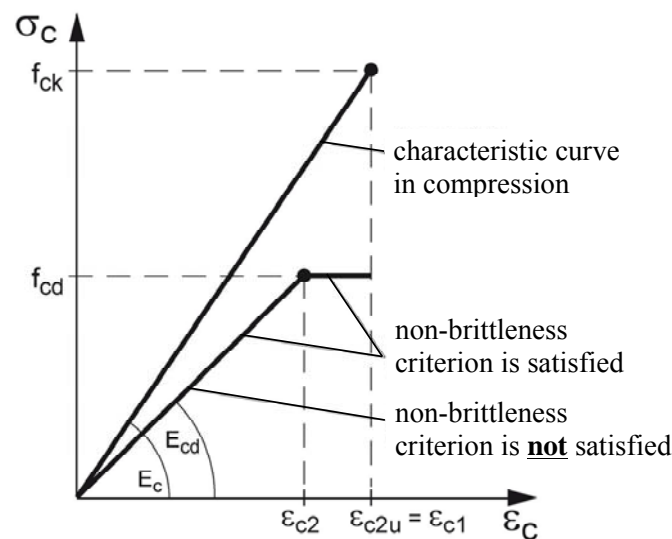
Figure 1: Stress-strain relationship in compression [2]

As for normal (NSC) and high strength concrete (HSC), the inclination of the stress-strain curve is reduced with respect to the mean value of the modulus of elasticity obtained from tests. This reduction may consider affects of creep and lower compressive strength. The proposed design value of the modulus of elasticity is given by Eq. (1) [2].

$$E_{cd} = E_{cm} / 1.3 \tag{1}$$

In Eq. (1), E_{cm} is the mean value of the modulus of elasticity obtained from tests. It is typically in the range of 45,000 to 55,000 N/mm². Using very stiff aggregates, such as bauxite, it can be significantly increased to up to 70,000 N/mm². A distinction between secant and tangent modulus is obsolete for UHPFRC. The strain ε_{c2} at ultimate load can be derived from the design values of the concrete compressive strength and the modulus of elasticity:

$$\varepsilon_{c2} = f_{cd} / E_{cd} \tag{2}$$

The design value of the concrete compressive strength can be determined acc. to Eq. (3).

$$f_{cd} = \alpha_{cc} \cdot f_{ck} / (\gamma_c \cdot \gamma_c') \tag{3}$$

where f_{ck} is the characteristic value of the cylinder compressive strength, γ_c is the partial safety factor for UHPFRC in compression, γ_c' is an additional partial safety factor for UHPFRC that has to be considered when necessary, and α_{cc} is the coefficient taking account of long term effects on the compressive strength and of unfavourable effects resulting from the way the load is applied. α_{cc} can be assumed to be equal to 0.85 [2].

The partial safety factors for NSC and HSC can conservatively be applied also to UHPFRC since investigations on the safety level for HSC showed that the variation coefficient of the compressive strength decreases for higher strength if an adequate quality standard is provided [3]. So, for high quality controlled processes, as is the rule for UHPFRC production, reduced partial safety factors (e. g. $\gamma_c = 1.3$ acc. to [2] or $\gamma_c = 1.35$ for precast concrete elements acc. to [4]) are appropriate. On the other hand, failure is very brittle and some kind of explosive for UHPFRC with very low fibre content. Thus, [2] suggests to distinguish in terms of safety level between "non-brittle" and "brittle" fracture behaviour. Only in the case that UHPFRC does not show a "non-brittle" behaviour, i. e. a behaviour equivalent to that of NSC, an additional partial safety factor $\gamma_c' = 1.2$ should be applied in Eq. (3). In addition, brittle failure should be assumed at the end of the ascending branch. This means that the stress-strain relationship ends for "brittle" UHPFRC when reaching the elastic limit strain ε_{c2} in Fig. 1.

"Non-brittle" behaviour can be achieved by adding a sufficient amount of fibres. In this case, the first linear-elastic stress-strain curve is extended by a plastic branch in order to account for the larger deformability. The end of the stress-strain relationship may then be assumed to be reached at a compression strain ε_{c2u} according to Eq. (5).

$$\varepsilon_{c2u} = f_{ck} / E_c \tag{5}$$

The plastic branch does not reflect the actual post-peak behaviour of UHPFRC. However, this is not a disadvantage, since the parameters required for the cross-sectional design are determined by integrating the stress-strain function (compare: parabola-rectangle diagram for normal and high strength concrete). The general limitation of the compression stress to a value $\varepsilon_{c2u} = \varepsilon_{c1}$ that has been verified by material testing (ε_{c1} = stress when reaching the ultimate load in the test) seems to be conservative.

2.2   Tensile loading

The tensile behaviour of UHPFRC is usually determined in axial tensile tests on prismatic specimens or, due to the more simple experimental procedure, derived from bending tests. To determine the matrix tensile strength, tests were performed on unnotched specimens while notched specimens are more meaningful to determine the behaviour in the cracked state.
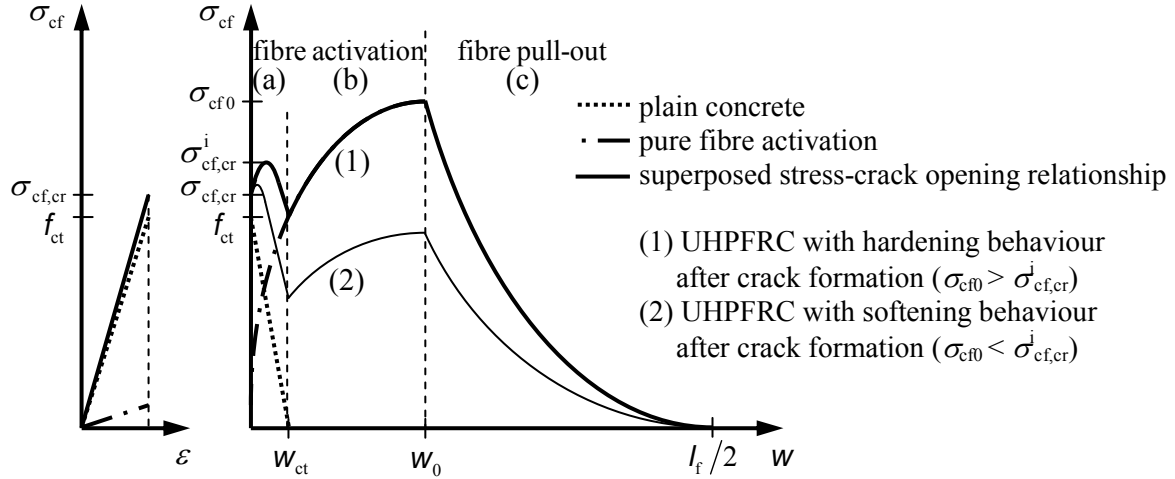
Figure 2: Schematic view of stress-strain (left) and stress-crack opening relationship (right) of UHPFRC under tensile loading [5]

The stress-strain relationship (Fig. 2, left) represents the behaviour of the continuum. There, the fibres participate in load bearing according to the ratio of their axial stiffness to the overall stiffness of the specimen. The tensile behaviour of a local cross section after crack initiation is separately shown in Fig. 2, right, using a stress-crack opening relationship which is considered to be more appropriate as constitutive law in the cracked state. While the concrete matrix softens after reaching the tensile strength (in Fig. 2, right, represented by a linear decrease of matrix tensile stress), the fibres are more and more activated with increasing crack opening. Due to the different bond length of the fibres on both sides of the crack, the nominal concrete tensile stress σ_{cf} transferred by the fibres (pure fibre activation) results in a root function acc. to Eq. (6) (for derivation see e. g. [6, 7]). Here, a constant friction stress is assumed (rigid-plastic bond law).

$$\sigma_{cf} = \sigma_{cf0} \cdot \left(2 \cdot \sqrt{w/w_0} - w/w_0 \right) \tag{6}$$

In Eq. (6), σ_{cf0} is the fibre efficiency (ultimate tensile stress in the cracked state), w is the actual crack width (w = 0 for unloaded state after appearance of crack), and w_0 is the crack width when reaching σ_{cf0}.

Equation (6) provides a strong increase of σ_{cf} at small crack widths. Superposition with the stresses of the softening matrix often results in an overall hardening behaviour (phase (a) in Fig. 2), which can also be observed in well arranged tests. This means that a stable micro-crack growth is initiated and macro cracking finally starts at a higher stress level $\sigma^i_{cf,cr}$.

Reaching σ_{cf0} in state II marks the transition from the phase of fibre activation to the phase of fibre pull-out. Henceforth, even the fibre with the largest possible embedment length, i. e. a

4

fibre crossing the crack perpendicularly at the middle of its length, shows slip on its entire embedment length. With further crack opening, all fibres are gradually pulled out from the matrix at the side with their shorter embedment length. Through this, the individual embedment lengths of the fibres and the total number of fibres being still involved in the load transfer decrease continuously. Therefore, the decrease of σ_{cf} initially is strong while at large crack openings the majority of the fibres has already been pulled out completely at one side of the crack and therefore is not participating anymore. Thus, σ_{cf} will show only a slight decrease at large crack openings. These considerations lead to a quadratic decrease of the nominal concrete stress in the pull-out phase (for derivation see e. g. [6, 7]):

$$\sigma_{cf} = \sigma_{cf0} \cdot l_f^2 \Big/ \left(16 \cdot w_0^2\right) \cdot \left(1 - \sqrt{1 + 16 \cdot w_0 \Big/ l_f^2 \cdot \left(w - l_f/2\right)}\right)^2 \qquad (7a)$$

$$\sigma_{cf} = \sigma_{cf0} \cdot \left(1 - 2 \cdot w/l_f\right)^2 \qquad \text{(Simplification of Eq. (7a), neglecting elastic fibre elongation)} \qquad (7b)$$

where l_f is the fibre length.

For the case that all fibres are oriented exclusively parallel to tensile direction, an equation for determining σ_{cf0} can be derived due to theoretical considerations. It can be extended by semi-empirically deduced coefficients in order to consider the influence of fibre orientations deviating from tensile direction [6, 8]. However, due to numerous influencing parameters that can hardly be found analytically, it is recommended to determine σ_{cf0} experimentally.

Figure 3 shows that the typical stress-crack opening behaviour obtained in axial tensile tests on notched UHPFRC prisms can be approximated very well using Eqs. (6) and (7).
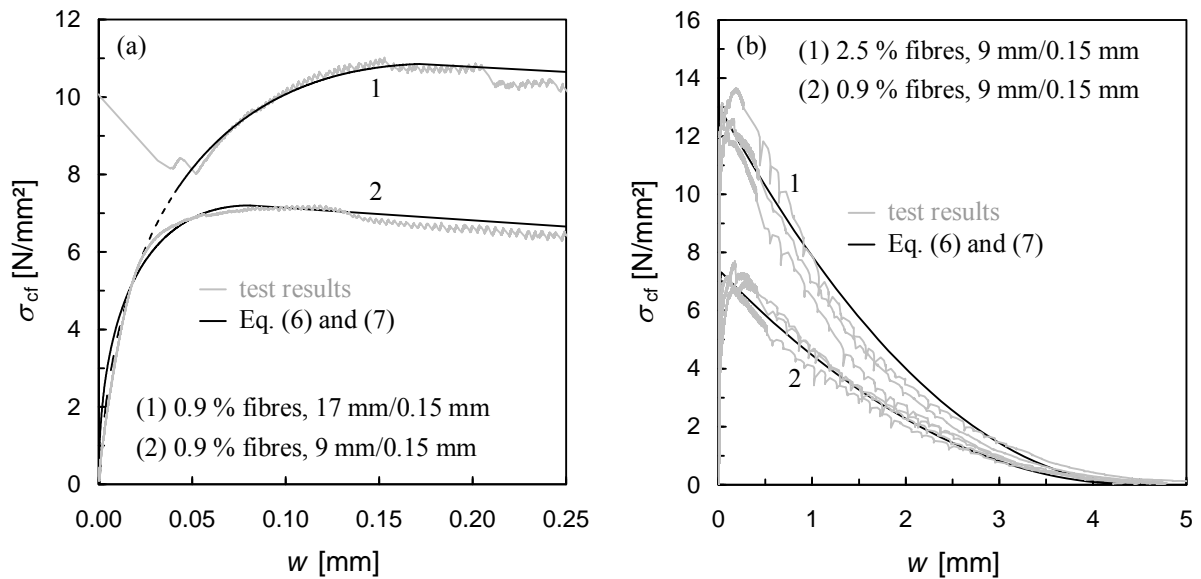
Figure 3: Approximation of the stress-crack opening behaviour of UHPFRC for small crack widths (left) and up to the complete pull-out of all fibres (right) [5]

Concerning cross-sectional design, uncracked state (state I) and cracked state (state II) are distinguished following the design philosophy of reinforced concrete. For checks in ultimate limit state (ULS), e. g. design for bending with/without axial force, cracked state has to be assumed in general and tensile strength of the matrix has to be neglected. This basic principle is adopted here also for UHPFRC which means that only tensile stresses transferred by the

reinforcement, i. e. the fibres, are considered in a cracked cross section. Matrix contributes only in compression. These traditional design assumptions (see also chapter 1) provide a consistent transition from reinforced concrete to fibre-reinforced concrete such as UHPFRC and also to UHPFRC with conventional reinforcement.

For cross-sectional design, the fibre efficiency in Eqs. (6) and (7) is represented by its design value σ_{cf0d} acc. to Eq. (8).

$$\sigma_{cf0d} = \alpha_{ct} \cdot \sigma_{cf0k} / \gamma_{cf} \qquad (8)$$

In Eq. (8), σ_{cf0k} is the characteristic value of the fibre efficiency as obtained from test results using statistical evaluation, γ_{cf} is the partial safety factor for UHPFRC in tension, and α_{ct} is a coefficient taking account of long term effects on the fibre efficiency.

Since the effects of long term or repeated loading on σ_{cf0} are not investigated sufficiently so far, α_{ct} should be applied very carefully especially for not static loading.

3.   DESIGN FOR BENDING WITH/WITHOUT AXIAL FORCE

Difficulties appear in cross-sectional design when applying the constitutive models for UHPFRC and the well-known stress-strain relationships for concrete and prestressing steel to equilibrium analysis at state II since the contribution of the fibres in tension is represented by a stress-crack opening law and not by a stress-strain relationship.

Thus, an additional compatibility condition is introduced which demands that the relative displacements between bar reinforcement and concrete matrix on the one hand as well as between the fibres and the concrete matrix on the other hand must cause the same slip or crack width, respectively. Thereby, it is possible to transfer the stress-crack opening relationship into a stress-strain relationship and to determine the distribution of tensile forces between bar reinforcement and fibres definitely. For checks in serviceability limit state (SLS), such as crack width limitation, this proceeding is essential in order to obtain meaningful results. The mechanical background to this is described in [7].

In design check for bending with/without axial force, the main interest however is to determine the bearing capacity of a cross section. The exact state of deformation of the cross section is only second-rank. In light of this, the following considerations will show that the problem most likely can be solved without careful consideration of compatibility. Nevertheless, a simple but satisfactory solution can be found. To this, Fig. 4 shows schematically the stress distributions and the resulting internal forces acting at the cracked cross section. Simplifying, the distribution of concrete compressive stresses does not consider the optional plastic branch.
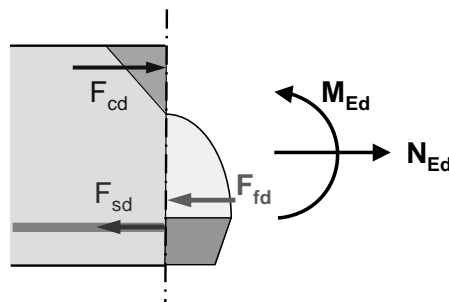
Figure 4: Stress distribution und resulting internal forces at a cracked cross section

For cross sections with rectangular compression zone, the resulting concrete compression force F_{cd} then acts at the third point from the top. The resulting steel force F_{sd} acts at the centre of gravity of the reinforcement. This couple of forces is complemented by the contribution of fibres in the cracked tensile zone. Since the matrix tensile strength is not considered in ULS (see chapter 2.2), the distribution of tensile stress transferred over the crack can be derived directly from the stress-crack opening relationship as a function of the actual crack width. Assuming that the crack width behaves linear over the depth of the tensile zone with $w = 0$ at the beginning of the tensile zone (analogy: plane cross section), then the concrete tensile zone represents a part of the stress-crack opening relationship acc. to Eqs. (6) and (7). In Fig. 4, this is exemplarily illustrated for the case that the crack width at the tensile edge of the cross section is about 1.5 times the crack width w_0. The resulting fibre force F_{fd} is obtained by integrating the fibre tensile stress.

In tests, a rapid increase of crack width at an approximately constant load level can be observed when reaching the yield stress of the reinforcement in a crack. Hence, in case that the crack width w_0 has not been reached already in the elastic range of the steel, the transition from the fibre activation to the fibre pull-out phase takes place at the latest immediately after onset of yielding. Thus, a minimum value of crack width $w = w_0$ can be assumed in the plastic range of the bar reinforcement. Assuming $w = w_0$ at the tensile edge of a rectangular cross section, the integration of Eq. (6) with the integration limits $w = 0$ and $w = w_0$ gives a shape factor of $\alpha_R = 0.83$. The distance between the neutral axis and the location of the resulting fibre force F_{fd} relating to the depth of the tensile zone then is $k_a = 0.56$ (see Fig. 5a).

$$F_{fd} = 0.83 \cdot (h - x) \cdot b \cdot \sigma_{cf0d}$$

$$F_{fd} = 0.81 \cdot (h - x) \cdot b \cdot \sigma_{cf0d}$$

a)   b)
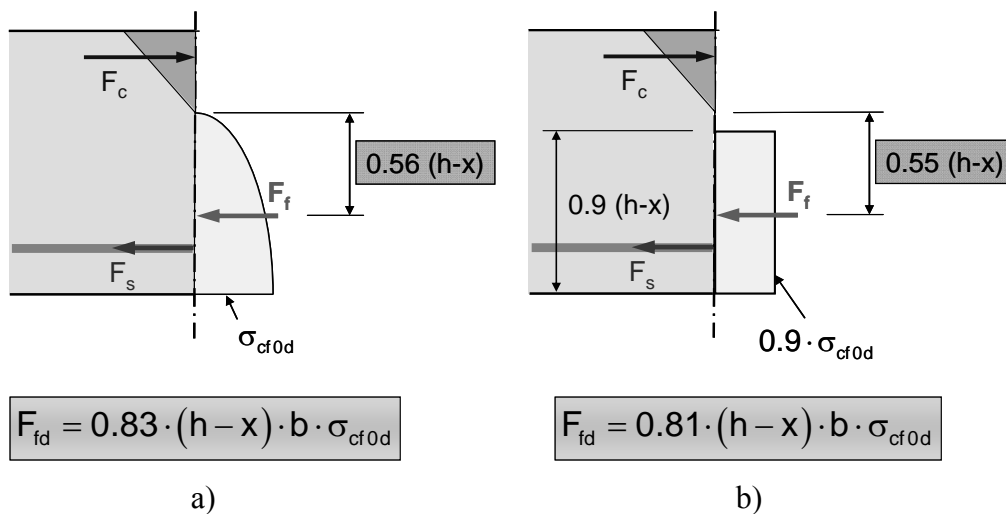
Figure 5: Stress distribution und resulting tensile force transferred by the fibres when reaching w_0 at the tensile edge; a) "realistic" stress distribution; b) "stress block" being equivalent to a)

Since the decrease of the stress-crack opening relationship in the phase of fibre pull-out ($w > w_0$) is significantly smaller than the increase in the phase of fibre activation ($w \leq w_0$), the factors α_R and k_a initially change only slightly with further crack opening and, in addition, in opposite directions. While the shape of the stress distribution converges to rectangle, the resulting fibre tensile force moves towards the centre of gravity of the tensile zone. This means that the resultant of the fibre tensile stress F_{fd} increases and the inner lever arm

decreases. For this reason, the bearing capacity is in general approximated very well assuming $w = w_0$ at the tensile edge of the cross section.

For cross-sectional design of NSC and HSC, the simple "rectangular stress distribution" [1] is favoured when doing hand calculation. Analogously, the more accurate stress distribution acc. to Fig. 5a for the fibre stress distribution in the tensile zone can be transferred to a "stress block" (Fig. 5b) that provides equivalent internal force and lever arm. The resulting values for F_{fd} are given in Fig. 5, where h and b are the total height and the width of the cross section, respectively, and x is the height of the concrete compression zone.

In order to not overestimate the fibre contribution in cases where the width of the cross section decreases in the direction of the tensile edge, it is recommended to substitute the value $0.9\ \sigma_{cf0d}$ in Fig. 5b by $0.85\ \sigma_{cf0d}$.

Regardless of the actual strain distribution across the height of the cross section, the stress at the compressive edge can simplifying be equated with f_{cd} acc. to Eq. (3).

With regard to the steel stress in the ultimate limit state a specific characteristic of combined reinforced cross sections has to be considered. For rebars with pronounced yield point, reaching the elastic limit is initially followed by a localisation of deformations in the critical crack. Hardening and further increase of steel stresses up to the steel tensile strength then takes place at already large crack widths corresponding with a sharp decrease of the tensile force carried by the fibres. Therefore, best fit for the bearing capacity is obtained when limiting the steel stress to the design value of the yield stress f_{yd}, i. e. hardening of the steel should be neglected. Alternatively, if hardening of the reinforcing steel up to the tensile strength is considered then the contribution of the fibres should be neglected because of the already very large crack widths in this case. Figure 6 gives an overview of the proposed simple model for cross-sectional design of UHPFRC for bending with/without axial force.

Legend:
k = 0.9
$\chi = 0.9$ in general
$\chi = 0.85$ if the width of the cross-section decreases towards the tensile edge
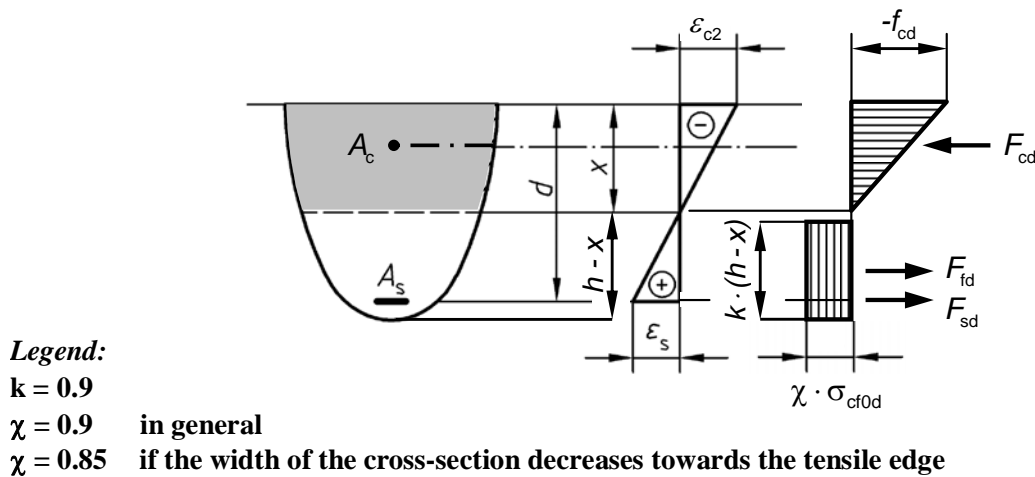
Figure 6: Proposed model for cross-sectional design of UHPFRC in bending

Based on Fig. 6, the following internal forces are obtained for rectangular cross sections:

$$F_{cd} = 0.5 \cdot b \cdot x \cdot f_{cd} \tag{9}$$

$$F_{sd} = A_s \cdot f_{yd} \tag{10}$$

$$F_{fd} = 0.81 \cdot b \cdot (h - x) \cdot \sigma_{cf0d} \tag{11}$$

In Eqs. (9) to (11), h and b are the total height and the width of the cross section, respectively, x is the height of the concrete compression zone, A_s is the cross-section area of the tensile reinforcement, and f_{yd} is the design value of the yield stress of the reinforcing steel.

The equilibrium conditions known from reinforced concrete can then be extended by the contribution of the fibres.

$$\Sigma H = 0 = N_{Ed} - F_{s1d} + F_{cd} - F_{fd} \qquad \text{(Equilibrium of forces)} \quad (12)$$

$$\Sigma M = 0 = M_{Eds} - F_{cd} \cdot (d - x / 3) + F_{fd} \cdot (d - 0.45 \cdot x - 0.55 \cdot h) \quad \text{(Moment equilibrium)} \quad (13)$$

If necessary, Eqs. (12) and (13) can be further extended in order to consider the contribution of reinforcing steel in the compression zone.

4.   COMPARISON BETWEEN PREDICTION OF THE PROPOSED MODEL AND TEST RESULTS

Stürwald [9] performed 4-point bending tests on UHPFRC beams. The test setup is shown schematically in Fig. 7. The beams had a rectangular cross section with the width b = 15 cm and the height h = 15 cm and h = 35 cm respectively. Most of them were reinforced with smooth straight steel fibres, l_f/d_f = 20 mm/0.25 mm, and with 3 up to 8 bars of reinforcing steel B 500, ϕ = 12 mm, or low ribbed high-strength steel St 1375/1570, ϕ = 10.5 and 11.5 mm. In tensile tests, yield stresses between 545 and 570 N/mm² were obtained for the rebars. The elastic limit of the high-strength steel was 1357 N/mm² (ϕ = 10.5 mm) and 1440 N/mm² (ϕ = 11.5 mm) respectively. The fibre efficiency of the UHPFRC mixtures was determined by axial tensile tests on notched prisms (cross section at the notch: 40 mm x 30 mm). Average values of 4.0 N/mm² (0.5 % steel fibres by vol., l_f/d_f = 20 mm/0.25 mm) and 10.3 N/mm² (1.5 % steel fibres by vol., l_f/d_f = 20 mm/0.25 mm) were obtained.
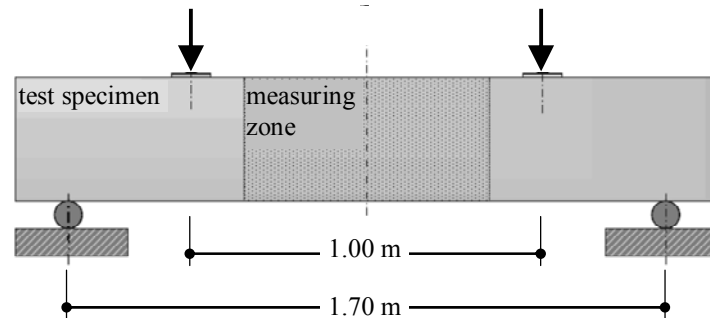
Figure 7: Sketch of the test setup for the bending tests on UHPFRC beams [9]

Table 1 shows the relevant geometry and material properties for 7 specimens as well as the ultimate bending moments M_{test} obtained in the tests. The ultimate bending moments M_{cal} predicted by the design model is indicated in the last row of Table 1. Calculation was done with mean values of the yield stress/elastic limit of the reinforcing steel (f_{ym}; $f_{p0,1m}$) as well as with mean values of the cylinder compressive strength of UHPFRC (f_{cm}). For the contribution of the fibres, it has been considered that the fibre orientation in the beams differs from that in the prisms and that, in addition, the fibre distribution shows some scatter within the measuring zone of the beams (range with constant bending moment). Thus, based on the evaluation of previous tests [7], the fibre efficiency at the critical crack was assumed to be only 70 % of the

9

mean value determined at the prisms, i. e. σ_{cf0k} = 2.8 N/mm² (0.5 % steel fibres by vol.) and σ_{cf0k} = 7.2 N/mm² (1.5 % steel fibres by vol.) where considered for the calculation.

Table 1: Geometry and material parameters of the test specimens and comparison between the test results [9] and the proposed model

name of the specimen	b [cm]	h [cm]	d [cm]	A_s [cm²]	f_{cm} [N/mm²]	σ_{cf0k} [N/mm²]	M_{test} [kNm]	M_{cal} [kNm]
H35-3St-F0	15	35	31.5	3.12[*]	192	-	138	137
H35-3St-F20-0,5	15	35	31.5	3.12[*]	211	2.8	167	157
H35-3St-F20-1,5	15	35	31.5	3.12[*]	189	7.2	179	186
H35-5St-F20-0,5	15	35	30.5	4.85[*]	184	2.8	223	219
H35-8BSt-F20-0,5	15	35	30.5	9.05[**]	181	2.8	174	170
H15-3St-F20-0,5	15	15	11.5	3.12[*]	207	2.8	50.1	50.4
H15-3BSt-F20-0,5	15	15	11.5	3.39[**]	207	2.8	26.6	25.1

reinforcing steel: [*] St 1375/1570 with $f_{p0,1m}$ = 1440 N/mm²; [**] B 500 with f_{ym} = 570 N/mm²

5.   CONCLUSIONS

Comparison of bearing capacity predicted by the proposed model and experimental data shows an overall good agreement. The divergence is at maximum of about 6 %. Even if the contribution of the fibres to the bearing capacity does not dominate when combined with conventional reinforcement, the relevance of fibres for avoiding brittle failure in compression and spalling as well as in serviceability range is substantial. For design in ULS, the proposed model provides results of sufficient accuracy with reasonable effort.

REFERENCES

[1] EN 1992-1-1, Eurocode 2: Design of concrete structures - Part 1-1: General rules and rules for buildings, English version, European Committee for Standardization (CEN), December 2004.

[2] Fédération Internationale du Béton (fib), Task Group 8.6, 'Draft of Bulletin on Ultra High Performance Fiber Reinforced Concrete', November 2011 (unpublished).

[3] Tue, N. V., Schenck, G. and Schwarz, J., 'Absicherung der statistisch erhobenen Festbetonkennwerte für die neue Normengeneration', Research Report (Institut für Massivbau und Baustofftechnologie, University of Leipzig, 2005).

[4] DIN EN 1992-1-1/NA:2011-01, National Annex (Germany) – Nationally determined parameters – Eurocode 2: Design of concrete structures – Part 1-1: General rules and rules for buildings, Normenausschuss Bauwesen (NABau) im DIN, Beuth Verlag GmbH, Berlin, January 2011.

[5] Leutbecher, T. and Fehling, E., 'Tensile Behavior of Ultra-High-Performance Concrete Reinforced with Reinforcing Bars and Fibers: Minimizing Fiber Content', *ACI Structural Journal* **109** (2) (2012), Farmington Hills, MI.

[6] Pfyl, T., 'Tragverhalten von Stahlfaserbeton', Doctoral Thesis (ETH Zürich, No. 15005, 2003).

[7] Leutbecher, T., 'Rissbildung und Zugtragverhalten von mit Stabstahl und Fasern bewehrtem Ultrahochfesten Beton (UHPC)', Doctoral Thesis, *Structural Materials and Engineering Series* **9** (kassel university press GmbH, Kassel, 2008).

[8] Voo, J. Y. L. and Foster, S. J., 'Variable Engagement Model for Fibre Reinforced Concrete in Tension', Uniciv Report No. R-420 (The University of New South Wales, 2003).

[9] Stürwald, S., 'Versuche zum Biegetragverhalten von UHPC mit kombinierter Bewehrung', Research Report (Chair of Concrete Structures, Department Civil Enginieering, University of Kassel, 2011).